Atmos. Chem. Phys. Discuss., 13, 5601–5648, 2013
www.atmos-chem-phys-discuss.net/13/5601/2013/
doi:10.5194/acpd-13-5601-2013

Atmospheric Chemistry and Physics
Open Access
Discussions

Global sea-to-air flux climatology for bromoform, dibromomethane and methyl iodide

F. Ziska[1], B. Quack[1], K. Abrahamsson[2], S. D. Archer[3], E. Atlas[4], T. Bell[5], J. H. Butler[6], L. J. Carpenter[7], C. E. Jones[7,*], N. R. P. Harris[8], H. Hepach[1], K. G. Heumann[9], C. Hughes[10], J. Kuss[11], K. Krüger[1], P. Liss[12], R. M. Moore[13], A. Orlikowska[11], S. Raimund[14,], C. E. Reeves[12], W. Reifenhäuser[15,***], A. D. Robinson[8], C. Schall[16], T. Tanhua[1], S. Tegtmeier[1], S. Turner[12], L. Wang[17], D. Wallace[13], J. Williams[18], H. Yamamoto[19,****], S. Yvon-Lewis[20], and Y. Yokouchi[19]**

[1]GEOMAR, Helmholtz-Zentrum für Ozeanforschung Kiel, Kiel, Germany
[2]Department of Analytical and Marine Chemistry, Chalmers University of Technology and Gothenburg University, Gothenburg, Sweden
[3]Plymouth Marine Laboratory, Plymouth, PMI, Plymouth, UK now at Bigelow Laboratory of Ocean Sciences, USA
[4]Marine and Atmospheric Chemistry, Rosenstiel School of Marine and Atmospheric Science, University of Miami, MAC, Miami, USA
[5]Department of Earth System Science, University of California, UCI, Irvine, USA

[6]Earth System Research Laboratory, Global Monitoring Division, ESRL/NOAA, Boulder, USA
[7]Department of Chemistry, University of York, York, YO10 5DD, UK
[8]Department of Chemistry, University of Cambridge, Cambridge, CB2 1EW, UK, Cambridge, UK
[9]Institut für Anorganische Chemie und Analytische Chemie, Johannes Gutenberg-Universität, JGU, Mainz, Germany
[10]Laboratory for Global Marine and Atmospheric Chemistry, University of East Anglia, LGMAC/UEA, Norwich, UK
[11]Institut für Ostseeforschung Warnemünde, IOW, Rostock-Warnemünde, Germany
[12]School of Environmental Science, University of East Anglia, Norwich, UK
[13]Department of Oceanography, Dalhousie University, Halifax, B3H 4R2, Canada
[14]CNRS, UMR 7144, Equipe Chim Marine, Stn Biol Roscoff, 29680 Roscoff, France
[15]Bayerisches Staatsministerium für Umwelt und Gesundheit, Augsburg, Germany
[16]Fresenius Medical Care Deutschland GmbH, Frankfurterstrasse 6–8, 66606 St. Wendel, Germany
[17]Rutgers State University of New Jersey, New Brunswick, USA
[18]Max Planck Institute for Chemistry, Air Chemistry Department, MPI, Mainz, Germany
[19]National Institute for Environmental Studies, Tsukuba, Ibaraki 305-0053, Japan
[20]Department of Oceanography, Texas A&M University, College Station, USA
[*]now at: Graduate School of Global Environmental Studies, Kyoto University, Yoshida-Honmachi, Sakyo-ku, Kyoto 606-8501, Japan
[**]now at: GEOMAR, Helmholtz-Zentrum für Ozeanforschung Kiel, Kiel, Germany
[***]now at: Bayerisches Landesamt für Umwelt, Augsburg, Germany
[****]now at: Marine Works Japan, Ltd., Oppamahigashi, Yokosuka 237-0063, Japan

Received: 13 December 2012 – Accepted: 7 February 2013 – Published: 27 February 2013

Correspondence to: F. Ziska (fziska@geomar.de)

Published by Copernicus Publications on behalf of the European Geosciences Union.

Abstract

Volatile halogenated organic compounds containing bromine and iodine, which are naturally produced in the ocean, are involved in ozone depletion in both the troposphere and stratosphere. Three prominent compounds transporting large amounts of marine halogens into the atmosphere are bromoform ($CHBr_3$), dibromomethane (CH_2Br_2) and methyl iodide (CH_3I). The input of marine halogens to the stratosphere is based on observations and modeling studies using low resolution oceanic emission scenarios derived from top down approaches. In order to improve emission inventory estimates, we calculate data-based high resolution global sea-to-air flux estimates of these compounds from surface observations within the HalOcAt database (https://halocat.geomar.de/). Global maps of marine and atmospheric surface concentrations are derived from the data which are divided into coastal, shelf and open ocean regions. Considering physical and biogeochemical characteristics of ocean and atmosphere, the open ocean water and atmosphere data are classified into 21 regions. The available data are interpolated onto a $1^\circ \times 1^\circ$ grid while missing grid values are interpolated with latitudinal and longitudinal dependent regression techniques reflecting the compounds' distributions. With the generated surface concentration climatologies for the ocean and atmosphere, global concentration gradients and sea-to-air fluxes are calculated. Based on these calculations we estimate a total global flux of $1.5/2.5\,\mathrm{Gmol\,Br\,yr^{-1}}$ for $CHBr_3$, $0.78/0.98\,\mathrm{Gmol\,Br\,yr^{-1}}$ for CH_2Br_2 and $1.24/1.45\,\mathrm{Gmol\,I\,yr^{-1}}$ for CH_3I (Robust Fit/Ordinary Least Square regression technique). Contrary to recent studies, negative fluxes occur in each sea-to-air flux climatology, mainly in the Arctic and Antarctic region. "Hot spots" for global polybromomethane emissions are located in the equatorial region, whereas methyl iodide emissions are enhanced in the subtropical gyre regions. Inter-annual and seasonal variation is contained within our calculations for all three compounds. Compared to earlier studies, our global fluxes are at the lower end of estimates, especially for bromoform. An underrepresentation of coastal emissions and

of extreme events in our estimate might explain the mismatch between our bottom up emission estimate and top down approaches.

1 Introduction

Halogen (fluorine, chlorine, bromine, iodine) containing volatile organic compounds play an important role in tropospheric (Vogt et al., 1999; von Glasow et al., 2004) and stratospheric chemical cycles (Solomon et al., 1994; Salawitch et al., 2005). The ocean is the largest source of natural bromine and iodine containing halocarbons (Quack and Wallace, 2003; Butler et al., 2007; Montzka and Reimann, 2011). When emitted into the atmosphere, these compounds, comprising mainly very short lived species (VSLS), having an atmospheric lifetime of less than 0.5 yr, contribute to the pool of reactive halogen compounds via photochemical destruction and reaction with hydroxyl radicals (von Glasow, 2008). Deep convection, especially in the tropics, can transport VSLS above the tropical tropopause layer (Aschmann et al., 2009; Tegtmeier et al., 2012) and into the stratosphere, where they influence stratospheric ozone destruction (Salawitch et al., 2005; Sinnhuber et al., 2009). Reactive bromine and iodine are more efficient in destroying stratospheric ozone than chlorine (e.g. Chipperfield and Pyle, 1998).

Recent studies have revealed a missing source of ~ 5 pptv inorganic bromine in the stratosphere, which could possibly be explained by the contribution of oceanic VSLS (Sturges et al., 2000; Sinnhuber and Folkins, 2006; Dorf et al., 2008). The absence of global emission maps of VSLS as input for Chemistry Transport Models (CTM) and Chemistry Climate Models (CCM) is a key problem for determining their role in stratospheric ozone depletion. The most widely reported short lived halogenated compounds containing bromine in both the atmosphere and the ocean are bromoform ($CHBr_3$) and dibromomethane (CH_2Br_2). Together, they may contribute ~ 15–40 % to stratospheric bromine (Montzka and Reimann, 2011), with $CHBr_3$ is considered to be the largest single source of organic atmospheric bromine (Penkett et al., 1985) to the atmosphere. Its production involves marine organisms such as macro algae and phytoplankton

(Gschwend et al., 1985; Nightingale et al., 1995; Carpenter and Liss, 2000; Quack et al., 2004). CH_2Br_2 is formed parallel to the biological $CHBr_3$ formation in seawater (Manley et al., 1992; Tokarczyk and Moore, 1994) and, therefore, generally correlates with oceanic and atmospheric bromoform (e.g. Yokouchi et al., 2005; O'Brien et al., 2009), although it occasionally shows a different pattern in the deeper ocean indicating its different cycling in the marine environment (Quack et al., 2007b). Large variability in the $CH_2Br_2 : CHBr_3$ ratio has been observed in sea water and atmosphere, while elevated concentrations of both compounds in air and water are found in coastal regions, close to macro algae and around islands, as well as in oceanic upwelling areas (Yokouchi et al., 1997, 2005; Carpenter and Liss, 2000; Quack and Wallace, 2003; Quack et al., 2007a). Seasonal variations have been observed in coastal regions (Archer et al., 2007; Orlikowska and Schulz-Bull, 2009), however the database is insuffient to resolve a temporal dependence. Anthropogenic sources, such as water chlorination, are locally significant, but relatively small on a global scale (Quack and Wallace, 2003). The uncertainties in the natural source strengths are high, both on the process level and for the global oceanic emission flux.

Atmospheric modeling studies have derived top down global estimates of between 5.4–7 $\mathrm{Gmol\,Br\,yr^{-1}}$ for bromoform and between 0.7–1.4 $\mathrm{Gmol\,Br\,yr^{-1}}$ for dibromomethane using different atmospheric transport models (Warwick et al., 2006; Kerkweg et al., 2008; Liang et al., 2010; Ordonez et al., 2012). Global bottom up emission estimates based on the interpolation of surface atmospheric and oceanic measurements have yielded emission estimates of between 2.8–10.3 $\mathrm{Gmol\,Br\,yr^{-1}}$ for $CHBr_3$ and between 0.8–3.5 $\mathrm{Gmol\,Br\,yr^{-1}}$ for CH_2Br_2 (Carpenter and Liss, 2000; Yokouchi et al., 2005; Quack and Wallace, 2003; Butler et al., 2007). Additionally a parameterization for oceanic bromoform concentrations covered by a homogenous atmosphere estimates a flux of 1.45 $\mathrm{Gmol\,yr^{-1}}$ for $CHBr_3$ between 30° N–30° S (Palmer and Reason, 2009).

Methyl iodide is mainly emitted from the ocean and is characterized as a dominant gaseous organic iodine species in the troposphere (Carpenter, 2003; Yokouchi et al., 2008). This compound is involved in important natural iodine cycles and in several atmospheric processes such as stratospheric ozone loss and formation of marine aerosol (Solomon et al., 1994; McFiggans et al., 2000). Enhanced oceanic concentrations of CH_3I are found in coastal areas where marine macro algae have been identified as the dominant coastal CH_3I source (e.g. Manley and Dastoor, 1988; Manley et al., 1992; Manley and delaCuesta, 1997; Laturnus et al., 1998; Bondu et al., 2008). Phytoplankton, bacteria and non-biological pathways, such as photochemical degradation of dissolved organic carbon, are significant open ocean sources (Happell and Wallace, 1996; Amachi et al., 2001; Richter and Wallace, 2004; Hughes et al., 2011). Terrestrial sources, such as rice paddies and biomass burning, are suggested to contribute 30 % to the total atmospheric CH_3I budget (Bell et al., 2002). Modeling studies and data interpolation estimate global CH_3I emissions between 2.4–4.3 $\mathrm{Gmol\,I\,yr^{-1}}$ (Bell et al., 2002; Butler et al., 2007; Ordonez et al., 2012). Smythe-Wright et al. (2006) extrapolated a laboratory culture experiment with *Prochlorococcus marinus* (kind of picoplankton) to a global CH_3I emission estimate of 4.2 $\mathrm{Gmol\,I\,yr^{-1}}$, whereas the study of Brownell et al. (2010) disputed the result of Smythe-Wright et al. (2006) and suggest that *P. marinus* is not significant on a globally scale.

This study presents the first global 1° × 1° climatological concentration and emission maps for the three important VSLS (bromoform, dibromomethane and methyl iodide) based on atmospheric and oceanic surface measurements available from the HalOcAt (Halocarbons in the ocean and atmosphere) database project (https://halocat.geomar.de/). According to current knowledge of the compounds distribution and possible sources, we classify the data based on physical and biogeochemical characteristic of the ocean and atmosphere. The interpolation of the missing values onto the 1° × 1° grid with two different regression techniques is analyzed. Based on the generated marine and atmospheric surface concentration maps, global climatological emissions are calculated with a commonly used sea-to-air flux parameterization applying temporally highly resolved wind speed, sea surface temperature, salinity and pressure data. The results are compared to estimates of other studies and the temporal and spatial variability of the climatological sea-to-air flux is discussed. The aim of this study is to provide improved global sea-to-air flux maps based on in situ measurements and on known physical and biogeochemical characteristic of the ocean and atmosphere in order to reduce the uncertainties in modeling the contribution of VSLS to the stratospheric halogen budget.

2 Data

In this study, $CHBr_3$, CH_2Br_2 and CH_3I data are extracted from the HalOcAt database (https://halocat.geomar.de/ see Supplement for a list of the used data). The database currently contains about 200 contributions, comprising roughly 55 400 oceanic and 476 000 atmospheric measurements from a range of oceanic depths and atmospheric heights of 19 different halocarbon compounds (mainly very short-lived brominated and iodinated trace gases) from 1989 to 2011. Coastal stations, ship operation and aircraft measurements are mainly within the database. The individual data sets are provided by the dataset creators. Since the compounds distribution is too variable and the current data is too sparse to identify a robust criterion for quality check and data selection, no overall quality and intercalibration control on the database exists. Future work is planned to use common standards and perform laboratory intercalibrations (Butler et al., 2010; Jones et al., 2011). Thus, we use all available surface ocean values to a maximum depth of 10 m (5300 data points) and atmospheric values to a maximum height of 20 m (4200 data points) from the year January 1989 until August 2011 (Fig. 1) for the calculation of the climatological concentrations. For sea-to-air flux calculations (see Sect. 3.6), 6 hourly means of wind speed (U), sea level pressure (SLP) and sea surface temperature (SST) are extracted from the ERA-Interim meteorological assimilation database (Dee et al., 2011) for the years 1989–2011 ($1^\circ \times 1^\circ$), whereas salinity (SSS) is taken from the World Ocean Atlas 2009 (Antonov et al., 2010).

3 Methodology

3.1 Approach

The high variability of VSLS (especially for $CHBr_3$) in both ocean and atmosphere is not explicable with any correlation to common parameterization. Production pathways with associated production rates and reliable proxies for the compounds distributions are not available. We tried correlations, multiple linear regressions and polynomial fits with biological and physical parameters (e.g. chlorophyll *a*, SST, SSS, SLP, mixed layer depth) to interpolate the data. Since none of the techniques provided satisfying results, we choose to simplify our approach. In order to compute climatological concentration maps, information on the compounds distributions is extracted from the existing data sets of the HalOcAt database and the literature on source distributions. Both surface ocean and atmospheric $CHBr_3$ concentrations are generally higher in productive tropical regions, at coast lines and close to islands, while generally lower and more homogeneous concentrations are located in the open ocean (Fig. 1). The global ocean shows a latitudinal and longitudinal variation of biological regimes, driven by circulation and regionally varying nutrient input as well as light conditions. Productive eastern boundary upwelling, equatorial and high latitudinal areas are separated by low productive gyre regions. We therefore separated the ocean in different latitudinal bands and applied (multiple) linear regressions between the compounds distribution and latitude and longitude (see more details in Sect. 3.4). The linear regressions reflect the underlying coarse distribution of the data and their longitudinal and latitudinal concentration dependence within different biogeochemical and physical regimes appears as current best available approach for data analysis and interpolation. This approach is independent of additional variables, reasonably reflecting the current knowledge about the compounds distribution considering different biogeochemical oceanic regions and minimizes the creation of non-causal characteristics. The existing data are interpolated onto a $1^\circ \times 1^\circ$ grid. The missing grid values are filled with the latitudinal and longitudinal dependent regression techniques. With the climatological oceanic and atmospheric surface concentration maps, global concentration gradients and sea-to-air fluxes are calculated.

3.2 Classification

Considering the compounds distribution, all data are divided into coastal, shelf and open ocean regimes (coastal and shelf areas are neighboring on the 1° × 1°, while the other grid points belong to the open ocean water and atmosphere regime).

The open ocean water data are further divided into 4 regions for each hemisphere. The inner tropics (0 to 5°) include the equatorial upwelling regions with high biomass abundance and elevated $CHBr_3$ concentrations, especially in the eastern ocean basins. The subtropical gyres, with descending water masses and, hence low biological production at the surface, are identified as the second region (5 to 40°). The third region comprises the temperate zones between 40 to 66° with higher climatological surface chlorophyll concentrations than in the gyre region and increasing $CHBr_3$ concentrations towards higher latitudes. The fourth region (poleward of 66°) encompasses the polar Arctic and Antarctic with colder surface waters and occasional ice cover.

The open ocean atmosphere is classified in a slightly different way from that of the open ocean waters. The inner tropical region (here from 0 to 10°) is characterized by the intertropical convergence zone (ITCZ), upward motion, low pressure and deep convection. Additionally, each hemisphere is divided into 3 wind regimes: subtropics (10 to 30°), mid-latitudes (30 to 60°) (westerlies, storm tracks) and polar regions (60 to 90°), characterized by distinctive air masses, wind directions and weather conditions.

The open ocean regimes (oceanic and atmospheric) are further subdivided into the Atlantic, Pacific, Indian and Arctic basins. Thus the HalOcAt data is sorted into 21 different regions for surface open ocean water and atmosphere (see Tables S1 and S2 in the Supplement). Gridding the data and inserting missing values is described in the following section. The data classification for dibromomethane, which has been reported to have similar source regions as $CHBr_3$ (Yokouchi et al., 2005; O'Brien et al., 2009) and for methyl iodide with coastal, planktonic and photochemical sources (Hughes et al., 2011; Moore et al., 1994; Richter and Wallace, 2004), has been linked to the one described for $CHBr_3$. The data density for dibromomethane and methyl iodide is equivalent to that of bromoform (Fig. 1).

3.3 Objective mapping

The original, irregular measurements are transferred to a uniform global 1° × 1° grid point using a Gaussian interpolation. Based on this technique the value at each grid point is calculated with the measurements located in the defined Gaussian range around the respective grid point. The Gaussian Bell area can be wider (3°) for the surface open ocean water and atmosphere data than for the coast or shelf region (1°) because of the homogeneity of data in the open ocean regions. This kind of interpolation takes the spatial variance of the measurements into account. The smaller the distance between a given data point and the grid point, the greater it is weighting in the grid point calculation (Daley, 1991). For grid points where no measurements are available within the Gaussian Bell area no concentration data can be calculated directly and a linear regression needs to be applied.

3.4 Linear regression

Data gaps on the 1° × 1° grid are filled based on a multiple linear regression technique using the original dataset, applying the functional relationship between latitude and longitude as predictor variables, x_1 and x_2, and compound concentration as the response variable, y (Fig. 2, for specific details see Sect. 3.5).

The regression coefficients for each defined oceanic and atmospheric region are given in Tables S1 and S2 in the Supplement. For regions where the spatial coverage of the data is extremely poor a first order regression based on the latitude variable only is used. For regions without data or in case the interpolation does not produce reasonable results (e.g. concentrations calculated with the regression are negative), the linear regression of neighboring open ocean regions of the same latitudinal band is used to fill the data gaps, assuming similar physical and biogeochemical conditions. For example, no data exist for the tropical Indian Ocean (0–5° N), thus, open ocean data from the tropical Atlantic and Pacific (0–5° N) are used to determine the missing values. Since data coverage in coastal and shelf regions is low the regression coefficients are calculated over each entire hemisphere. Additionally, we apply the Root Mean Square Error (RMSE), calculated as the difference between the predicted values and the observed data, as measure for accuracy. A small RMSE reflects a low bias and variance of the predicted values, with zero indicating that the regression techniques predict the observations perfectly.

3.5 Robust fit vs. ordinary least square

In our study, two different regression techniques are applied. The Ordinary Least Square (OLS) technique contains the least squares method. This means that the sum of squared vertical deviations between the empirical *y*-values in the dataset and the predicted linear approximation is minimized.

The second method for calculating regression coefficients is the Robust Fit (RF) technique which excludes extreme data. The most common general method of robust regression is the "M-estimation", introduced by Huber (1964). A robust estimation is based on the quantity of measurements and the influence of distant data points is reduced approximately to zero with increasing deviance. A regression analysis is robust if it is not sensitive to outliers.

Both regression methods are shown in Fig. 2 for all latitudinal divided open ocean water and atmospheric measurements for bromoform. The RF regression lines (red) are lower than the OLS (black) and occasionally show different trends. The reason for the large deviation between the RF and OLS regression is the different weighting of outliers. Outliers crucially influence the value of the OLS slope, whereas the RF regression is located at the largest data density and reduces the influence of outliers.

While the RF captures background values, the OLS technique indicates the variability of the data. Based on these concentration maps, global fluxes are calculated and compared to literature values.

3.6 Air-sea gas exchange and input parameters

Fluxes (F) across the sea-air interface are generally calculated as the product of the sea-to-air concentration difference and a gas exchange velocity. The partitioning of a gas between the water and gas phase is described by the dimensionless Henry's law constant (H) which highly depends on temperature and the molecular structure of the species. For our calculations, the Henry's law constants of Moore et al. (1995a,b) are used. The atmospheric mixing ratios are converted to equilibrium water concentrations (C_a) and the deviation from the actual measured water concentration (C_w) describes the driving concentration gradient. The sea-to-air flux is negative if the transport is from the atmosphere to the ocean.

$$F = k(C_\mathrm{w} - C_\mathrm{a}\, H^{-1}) \tag{1}$$

Several parameterizations for the air-sea gas exchange exist in the literature, which express the relationship between the gas exchange velocity (k) and wind speed (e.g. Liss and Merlivat, 1986; Wanninkhof,1992; Wanninkhof and McGillis,1999; Nightingale et al., 2000). Experiments have shown that the dominant parameter influencing k is the wind speed (U). We chose to calculate the transfer coefficients based on the parameterization from Nightingale et al. (2000) with corrections for the water temperature and a Schmidt number (Sc) dependence for each gas (Quack and Wallace, 2003; Johnson, 2010).

$$k = (0.222U^2 + 0.333U)\sqrt{(660Sc^{-1})} \tag{2}$$

The Schmidt number is the ratio of the diffusion coefficient of the compound of interest and the kinematic viscosity of sea water and depends mainly on the temperature and the salinity.

The gas exchange velocity and concentration gradient are dependent on SST, SSS, U and SLP as input parameters. During the initial stages of this study, we used climatological mean values (1989–2011) of the input parameters for our calculation of the global climatological emission estimates. A sensitivity study demonstrates how changes in the input parameters (climatological means) impact the global flux calculation for bromoform, dibromomethane and methyl iodide (Fig. 3). Each input parameter is individually increased and decreased to $\pm 3\sigma$ (standard deviation) of its base value while holding the other input parameters fixed. The standard deviations are calculated for every grid point for the years 1989–2011. This study shows the importance of each input parameter for the flux variance. Sea surface salinity and sea level pressure affects the VSLS emission calculations least compared to the other parameters (Fig. 3). Changes in wind speed and sea surface temperature have strong influences on the bromoform sea-to-air flux. In general, a reduction/enhancement of the wind speed is directly accompanied by a decrease/increase of the air-sea gas exchange coefficients and higher/lower sea surface temperature lead to an increase/decrease of the concentration gradient as well as the air-sea gas exchange coefficients (Schmidt number). The dependencies of the global dibromomethane emission variability on the individual input parameters are the same as described for bromoform. The global methyl iodide emissions are mainly influenced by variations of the wind speed, while the other parameters have less impact. The sensitivity study shows that marginal changes of the input parameters can lead to a significant variation of the global flux estimate.

Averaging over a long time period when producing climatological means involves smoothing extreme values, which is especially relevant for the wind speed (Bates and Merlivat, 2001). Since the air-sea gas exchange coefficient has a non-linear dependence on wind speed, the application of averaged data fields causes a bias towards a lower flux when compared to using instantaneous winds and averaging the emission maps afterwards (Chapman et al., 2002; Kettle and Merchant, 2005). To reduce the bias, we apply the highest available temporal resolution of the input parameters and calculate 6 hourly global emissions with 6 hourly means of U, SST, SLP and monthly means for the SSS (from January 1989 to December 2011). Finally, we sum the emissions for each month, calculate monthly average emissions over the twenty-one years and summarize these twelve averages to obtain the climatological annual emission.

4 Results and discussion

Marine ($\text{pmol}\,\text{L}^{-1}$) and atmospheric (ppt) global surface concentration maps of bromoform, dibromomethane and methyl iodide calculated with the RF regression are shown in Fig. 4 (surface ocean concentrations and mixing ratios calculated with the OLS technique are illustrated in the Supplement). Based on the RF and OLS marine and atmospheric concentration maps, global sea-to-air flux climatologies are calculated (Fig. 5).

4.1 Climatological concentration maps of $CHBr_3$ and CH_2Br_2

Marine surface concentrations of bromoform (Fig. 4) show higher values located in the equatorial region ($\sim 6\,\text{pmol}\,\text{L}^{-1}$), upwelling areas (e.g. the Mauritanian upwelling region $\sim 21\,\text{pmol}\,\text{L}^{-1}$), near coastal areas ($\sim 17$–$42\,\text{pmol}\,\text{L}^{-1}$) and in shelf regions ($\sim 8$–$32\,\text{pmol}\,\text{L}^{-1}$), consistent with macro algal and anthropogenic sources along the coast lines as well as biological sources in upwelling areas (Carpenter and Liss, 2000; Quack and Wallace, 2003; Yokouchi et al., 2005; Quack et al., 2007a; Liu et al., 2011). The coastal and shelf areas both show a positive latitudinal sea surface concentration gradient for bromoform and dibromomethane towards the polar regions. The coastal sea surface concentrations of bromoform are on average twice as high as in the shelf region. The open ocean generally has homogeneous concentrations between 0.5–$4\,\text{pmol}\,\text{L}^{-1}$. Lower values are located especially in the subtropical gyres (~ 0.5–$1\,\text{pmol}\,\text{L}^{-1}$), most distinct in the Atlantic, North Pacific and southern Indian Ocean.

Estimating global concentration maps based on an identified linear relationship is difficult in regions with sparse or missing data (e.g. Indian Ocean). Atlantic and Pacific Ocean data must be used to fill the data gap in the Indian Ocean, since no measurements exist there. Nevertheless, this approach seems reasonable, since oceanic and atmospheric data of the Pacific and Atlantic are similar to each other and the Indian Ocean is subject to the same physical effects of upwelling and downwelling occurring in these oceans. Thus, we expect similar concentrations as in the other oceans. One data set is available for the northern Indian Ocean (Yamamoto et al., 2001). The few measurements for bromoform in the Bay of Bengal are unusually high ($> 50\,\mathrm{pmol\,L^{-1}}$) for an open ocean area. We decided to not include these outliers in our analysis, since our method would possibly overestimate water concentrations in the entire northern Indian Ocean using these data. The high concentrations in the equatorial region (the product of the other two basins) are colocated with the likely elevated $CHBr_3$ and CH_2Br_2 concentration at the surface due to the prevalent upwelling season during the northeast monsoon, indicating higher productivity (Schott et al., 2002). The entire ocean, and especially the Indian and Arctic, are data poor, require further sampling and evaluation to improve the predictions. Atmospheric surface mixing ratios of bromoform show similar distribution patterns. Higher atmospheric mixing ratios are located in the equatorial regions (1–3 ppt), around coastlines (~ 1–10 ppt) and upwelling regions (10–17 ppt), as well as in the northern Atlantic (~ 12–21 ppt), while lower mixing ratios are found above the subtropical gyres (~ 0.2–0.8 ppt).

The global surface oceanic and lower atmospheric concentration maps of dibromomethane show similar distribution patterns as bromoform. Enhanced oceanic surface concentrations are located around the equatorial region ($\sim 6\text{–}9\,\mathrm{pmol\,L^{-1}}$), while low concentrations occur in the subtropical gyres ($1\text{–}2\,\mathrm{pmol\,L^{-1}}$), similar to the $CHBr_3$ distribution, but are higher than the $CHBr_3$ values. It is expected that CH_2Br_2 is elevated in the atmosphere relative to $CHBr_3$ distant from the coastal source regions, because it has a longer atmospheric lifetime than $CHBr_3$ (e.g. Brinckmann et al., 2012) ($CH_2Br_2 = 0.33$ yr, $CHBr_3 = 0.07$ yr, Warneck and Williams, 2012).

Elevated marine dibromomethane concentrations are found in the Southern Ocean ($4\text{–}6\,\mathrm{pmol\,L^{-1}}$). This area is characterized by several circumpolar currents separated by frontal systems, with seasonally varying ice coverage, and is known to experience enhanced biological production (Smith and Nelson, 1985). Sea-ice retreat and the onset of microalgae blooms have been related to an increase in marine surface bromocarbon concentrations (Hughes et al., 2009). However, the increase of CH_2Br_2 compared to $CHBr_3$ is currently not understood.

The climatological maps represent annual average values that may underestimate seasonal and short term variations. These variations currently cannot be reflected in the model, since knowledge about production processes and the influence of environmental values on the concentrations is incomplete.

4.2 Climatological concentration maps of CH_3I

The same classification and interpolation technique used for the bromocarbons reveal elevated marine and atmospheric concentrations of methyl iodide (2–9 pmol L^{-1}, 0.3–1.5 ppt) in the subtropical gyre regions of both hemispheres (Fig. 4). This is in contrast to the oceanic concentration maps of bromoform and dibromomethane, and is in agreement with reported production processes, such as photochemical oxidation of dissolved organic matter and iodide, as well as production from cyanobacteria (e.g. Richter and Wallace, 2004; Smythe-Wright et al., 2006).

Additionally, enhanced oceanic concentrations and atmospheric mixing ratios are found in the upwelling region off Mauritania and near the coastlines north of 40° ($\sim$ 9 pmol L^{-1}). Here in the region of offshore trade winds and dust export the atmospheric methyl iodide from the ocean may be supplemented by input from land sources (Sive et al., 2007) as elevated air concentrations have been noted to be associated with dust events (Williams et al., 2007). The sharp concentration increase towards the coast, as observed for bromoform and dibromomethane, does not exist for methyl iodide. The open ocean concentrations are generally higher than the coastal values, except for the Northern Hemisphere. The elevated coastal oceanic concentrations might be due to the occurrence of macro algae and anthropogenic land sources as reported in the literature or to elevated levels of dissolved organic material (DOM) (e.g. Manley et al., 1992; Bell et al., 2002). The polar regions show generally homogenous and low

Title Page
Abstract | Introduction
Conclusions | References
Tables | Figures
◀| |▶
◀ ▶
Back | Close
Full Screen / Esc
Printer-friendly Version
Interactive Discussion

concentrations of methyl iodide (Antarctic: ~ 0.3 ppt, ~ 1.5 pmol L^{-1}; Arctic: ~ 1 ppt and ~ 0.3 pmol L^{-1}).

4.3 Climatological emission maps of $CHBr_3$ and CH_2Br_2

Elevated bromoform fluxes from the ocean to the atmosphere are generally found close to coastlines, in equatorial and eastern boundary upwelling regions (e.g. the Mauritanian upwelling region) and a wide region of the southern Pacific (subtropical gyre). Very high sea-to-air fluxes (> 1500 $\text{pmol m}^{-2}\,\text{h}^{-1}$) also occur in the Bay of Bengal, the Gulf of Mexico, the North Sea and the East-Coast of North America.

The occurrence of enhanced emissions around coastlines coincides with higher sea water concentrations in high biological production areas and contributes about 67/78 (RF/OLS) % Br ($CHBr_3$) and around 22/24 % Br (CH_2Br_2) to the global emission, whereas the coast and shelf region covers only ~ 16 % of the world ocean. Most of the open ocean appears almost in equilibrium with the atmosphere, especially in the subtropical gyre regions. A flux from the atmosphere to the ocean is seen in the entire Southern Ocean, the northern part of the Pacific and in some parts of the North Atlantic (e.g. east of North America).

Our open ocean flux of $CHBr_3$ is about 25 % of the global sea-to-air flux estimate, which is in agreement with the 20 % calculated by Butler et al. (2007) and the 33 % of Quack and Wallace (2003). This underlines that the coast and shelf regions play a significant role in the global bromoform budget. The tropics (20° N to 20° S, including open ocean, shelf and coastal area) represent the region with the highest bromoform emissions of 44/55 % (Table 3). This is in agreement with the top down approach of 55.6 % between 20° N to 20° S published by Ordonez et al. (2012) and of 37.7 % for 10° N to 10° S from Liang et al. (2010). A decrease in the total emission towards the polar region is visible. Hence, the tropics are a "hot spot" for bromoform emissions.

Compared to the sea-to-air fluxes based on the RF analysis, the emissions using the OLS method show enhanced sea-to-air fluxes in the North Atlantic and all gyre regions, and an elevated sink in the Arctic region (Fig. 5). We estimate a global positive sea-to-air flux for $CHBr_3$ of ~2.06 Gmol Br yr^{-1} (RF); ~2.96 Gmol Br yr^{-1} (OLS) and a global sink, air-to-sea flux, for $CHBr_3$ of ~0.56 Gmol Br yr^{-1} (RF); ~0.47 Gmol Br yr^{-1} (OLS).

The global emission distribution of CH_2Br_2 is similar to $CHBr_3$ due to their common sources (Fig. 5). Differences between the distribution of source and sink regions and of CH_2Br_2 emissions calculated with the RF and OLS regression are less pronounced than those of $CHBr_3$. The Arctic Ocean mainly acts as a sink for atmospheric CH_2Br_2, most likely because of the low sea surface temperatures, low water concentrations and higher air concentrations. The Southern Ocean (south of 50° S) acts as a source to the atmosphere. The OLS based emissions show an enhanced source region in the southern Pacific due to elevated marine surface concentrations. We estimate a positive global CH_2Br_2 sea-to-air flux of ~0.89 Gmol Br yr^{-1} (RF); ~1.09 Gmol Br yr^{-1} (OLS) and an air-to-sea flux of ~0.12 Gmol Br yr^{-1} (RF); ~0.11 Gmol Br yr^{-1} (OLS).

Our total open ocean flux of 0.6–0.76 Gmol Br (CH_2Br_2) yr^{-1} is in agreement with the estimates of ~0.7 Gmol Br yr^{-1}given by Ko et al. (2003) and 0.6 Gmol Br yr^{-1} given by Butler et al. (2007). The coast and shelf regions play a minor role for the global CH_2Br_2 budget compared to the open ocean, which contributes ~77 % Gmol Br yr^{-1}. The global latitudinal CH_2Br_2 emission distribution is in rough agreement with the $CHBr_3$ emissions (Table 3). Enhanced source regions for the atmosphere are found in the tropical area contributing about 44/49 % between 20° N and 20° S. This is lower compared to the study of Ordonez et al. (2012) who calculated a contribution of 63.1 % from 20° N to 20° S. The CH_2Br_2 emissions decrease towards the polar regions.

4.4 Climatological emission maps of CH_3I

The global emissions of CH_3I reveal an opposite pattern compared to $CHBr_3$ and CH_2Br_2 (Fig. 5). The main difference is the enhanced emission in the subtropical gyre regions showing a different intensity in each ocean basin.

Equatorial upwelling regions, as well as the Arctic and Antarctic polar regions, are mostly in equilibrium. In comparison to $CHBr_3$ and CH_2Br_2, the global CH_3I sea-to-air fluxes are generally positive, indicating the larger supersaturations of the oceanic waters. The OLS regression shows the North Atlantic to be a very strong source region for atmospheric methyl iodide, which is due to the large data variability there. Coast and shelf regions transport only ~ 13 % of I (CH_3I) to the atmosphere. The open ocean contribution of 87 % is more than the estimate from Butler et al. (2007) of 50 % open ocean emissions of methyl iodide. Maybe the subtropical gyre regions are more distinctive source areas than in Butler et al. (2007). The southern tropics and subtropics represent the regions with the highest emission strength, decreasing towards the polar areas (Table 3). We calculate a global sea-to-air flux for CH_3I of ~ 1.24 $\mathrm{Gmol\,I\,yr^{-1}}$ (RF) and ~ 1.45 $\mathrm{Gmol\,I\,yr^{-1}}$ (OLS).

4.5 Evaluation of RF and OLS results

All subtropical regions, and especially the equator, show a large temporal and spatial variability in the data, which is reflected in the enhanced RMSE parameter (Tables S1 and S2 in the Supplement). The wide concentration ranges might be caused by real variations between sampling in different seasons, where the seasonally varying strength and expansion of upwelling (equatorial and coastal) (Minas et al., 1982; Hagen et al., 2001) and solar flux may cause different concentrations of the compounds.

The evaluation of the two regression methods shows that RF is more representative of a climatology, since it is calculating a regression independently of outliers and weighted by the data distribution. In comparison, the OLS regression weights outliers, and, hence considers extreme data and variability more than the RF method. The OLS regression represents an upper-limit of averages (Fig. 2). The global appearances of RF and OLS maps are not extremely different (see Supplement). Nevertheless, they introduce slight differences in the concentration gradients and in the sea-to-air flux climatologies.

The influence of the RF and the OLS regression for the global surface concentration distribution in atmosphere and ocean, which has consequences for the concentration gradient, is shown in Table 1 and Fig. 6. In general, the OLS technique calculates higher mean and median values, including the enhanced concentrations and outliers. Additionally, bromoform shows higher variance compared to the other compounds in both techniques and reflects the high data variability between coastal and open ocean bromoform concentrations. Further, the calculated concentration gradient using the OLS method exhibits stronger source (emission into the atmosphere) and weaker sink regions compared to RF, which is most pronounced for bromoform (Fig. 6). The OLS and RF distribution (mean, median and standard deviation) for dibromomethane and methyl iodide are in closer agreement compared to bromoform. The reason for this smaller difference between RF and OLS is the occurrence of less extreme values in the concentration gradients for CH_2Br_2 and CH_3I compared to $CHBr_3$. The global surface emissions of bromoform, dibromomethane and methyl iodide yield a similar spatial distribution with both techniques (Table 2).

4.6 Comparison of estimation methods

In the following section we compare our emission climatology with recently published estimates, including different calculation techniques (i.e. bottom up and top down approaches), as well as laboratory experiments (Table 6). The global bromoform emission estimates show the largest difference between the studies.

Warwick et al. (2006) modeled surface mixing ratios using different emission scenarios and fitted them to the available atmospheric measurements. These scenarios applied different global emission estimates, e.g. the bottom up estimate from Quack and Wallace (2003). The course resolution of 2.8° × 2.8° used in the Warwick study does not resolve the coastal areas well, which are thought to be the main source for bromoform. In addition the applied uniform interpolations do not reflect the actual conditions. In the results of Warwick et al. (2006), the coastlines further north and south of the tropics exhibit no enhanced atmospheric bromoform concentrations or emission to the atmosphere compared to the open ocean. This does not reflect the in situ measurements from the HalOcAt database. Based on the study of Pyle et al. (2011) the emission estimate of Warwick et al. (2006) is reduced and updated to atmospheric bromoform measurements in the area of Southeast Asia. Other model studies based on the ideas of Warwick et al. (2006), e.g. Kerkweg et al. (2008) show the same underestimation of coastal emissions in the extra tropics. In contrast, Liang et al. (2010) consider all coastlines with enhanced emissions in their scenario; furthermore the finer classification of their emission scenario compared with Warwick et al. (2006) is similar to our study. Another comparable classification (latitudinal bands, higher emissions in coastal regions) is used in the model (top down approach) by Ordonez et al. (2012), who parameterized oceanic polybromomethanes emissions based on a chlorophyll *a* (chl *a*) dependent source in the tropical ocean (20° N to 20° S). We also see the occurrence of enhanced bromoform, as well as dibromomethane emissions in tropical upwelling regions and in coastal regions, although a direct correlation between chl *a* and the VSLS compounds is not apparent from the observations (Abrahamsson et al., 2004; Quack et al., 2007b). Palmer et al. (2009) developed a parameterization for $CHBr_3$ based on chl *a* (between 30° N–30° S) and other parameters (mixed layer depth, sea surface temperature and salinity, wind speed). The correlation between his modeled values and observations is $r^2 = 0.4$ which reveals the deficiency of this method (and chl *a*).

In some studies local emission estimates are interpolated to a global scale. Interpolating near-shore emissions may significantly overestimate the global sea-to-air fluxes, since they generally include elevated coastal concentrations, which are not representative for the global ocean. Yokouchi et al. (2005) applied a coastal emission ratio of $CHBr_3/CH_2Br_2$ of 9 and a global emission of $0.76\,\mathrm{Gmol\,Br\,y^{-1}}$ for CH_2Br_2 (WMO 2003) to infer a global $CHBr_3$ flux estimate of $10.26 \pm 3.88\,\mathrm{Gmol\,Br\,yr^{-1}}$. O'Brien et al. (2009) followed the same method and interpolated local near-shore measurements in the region surrounding the Cape Verde to a global scale using an emission ratio $CHBr_3/CH_2Br_2 = 13$. The global fluxes from these studies are nearly four times higher than those calculated in our study. It is very likely that these fluxes are too high because they are calculated with concentrations interpolated from highly productive source regions.

Butler et al. (2007) and Quack and Wallace (2003) interpolated oceanic and atmospheric in situ measurements for global emission estimates. Butler subdivided the ocean into the main basins and calculated the fraction of each compound for each region as a percentage. Coastal areas are not considered. The extrapolation by Quack and Wallace (2003) contained most of the currently available published measurements and used a finer area classification into shore, shelf and open ocean regions as well as into latitudinal bands. Both bottom up approaches applied a coarse data interpolation compared to the classification and regression techniques used in this study and appear too high.

We calculate a global CH_2Br_2 sea-to-air flux of 0.77–0.98 $\mathrm{Gmol\,Br\,yr^{-1}}$ which is also in the lower (0.71–3.5 $\mathrm{Gmol\,Br\,yr^{-1}}$) range of the other estimates (Table 4), but is in much closer agreement compared to the other compounds. Reasons for the good agreement to recent studies could be the longer atmospheric life time of CH_2Br_2 and the lower variance of sea water values which cause a more homogenous global distribution.

Some earlier emission estimations for CH_3I range from 1.05–10.5 $\mathrm{Gmol\,I\,yr^{-1}}$, which are listed in the publication of Bell et al. (2002), who produced the first seasonal model simulation of global oceanic and atmospheric CH_3I surface concentrations. A low correlation between observations and modeled data was obtained ($r = 0.4$). The authors assumed a missing biological sink of CH_3I in the ocean that would have reduced their computed concentrations to better match the observations. Sink and source mechanisms for the formation of CH_3I are not fully understood, making it difficult to model CH_3I emissions based on source and sink parameterizations. In our study a global sea-to-air flux of 1.24–1.45 $\mathrm{Gmol\,I\,yr^{-1}}$ is estimated, which is within the lower range of earlier studies (Table 4). Our calculated climatology uses a larger dataset than the study of Bell et al. (2002). Ordonez et al. (2012) calculate a global CH_3I flux of the same magnitude as our study using a top down approach with a modified global chemistry model that includes bromine and iodine chemistry. Smythe-Wright et al. (2006) calculated a global flux of iodine from *Prochlorococcus marinus* of $\sim 4.18\,\mathrm{Gmol\,I\,yr^{-1}}$ based on measurements from two cruises. The latter study assumes that this phytoplankton species is the major marine source of atmospheric CH_3I. Smythe-Wright et al.'s assumption that the oceanic surface ($< 40^\circ$ N and S) is covered with CH_3I producing picoplankton might overestimate the global CH_3I sea-to-air flux. Calculations based on culture experiments from Brownell et al. (2010) demonstrate that *Prochlorococcus marinus* accounts only for 0.03 % of the global CH_3I budget and is not a globally significant source of CH_3I. Hughes et al. (2011) suggest different culture conditions as a possible explanation for the contradictory culture experiment findings. The bottle experiments of Richter and Wallace (2004) suggested a photochemical production pathway of CH_3I in open ocean water which might also explain our surface distribution (enhanced emissions in the subtropical gyre regions).

The comparison of our global sea-to-air fluxes with other global estimates shows the greatest discrepancy for bromoform. We have shown that bromoform levels are the most variable in the ocean and atmosphere, which is smoothed by the applied regression technique. Possibly, the underrepresentation of extreme values generates too small concentration gradients, which reduces our total emission estimate. Especially in coastal and shelf regions, the $1^\circ \times 1^\circ$ grid resolution cannot resolve these extreme concentrations and very likely leads to underestimated emissions there.

5 Variability of the climatological sea-to-air fluxes

We calculate global emission fields, using fixed oceanic concentrations and atmospheric mixing ratios and the highest available temporal resolution of the input parameters over the time period 1989–2011: 6 hourly means of U, SST, SLP and monthly means for the SSS. The global emissions of every time step are averaged over each month and the average monthly emissions are summed to the annual climatological emission. The climatologies thus include annual, seasonal and short timescale temporal variability.

5.1 Variability of the concentration data

The calculated global 1° × 1° maps of oceanic concentrations and atmospheric mixing ratios include in situ measurements from 1989–2011, illustrating a climatological year and covering the entire globe. Seasonally changing conditions, e.g. light and water temperature or biological species composition, which have an influence on the variability of the air and water concentrations in certain areas (Archer et al., 2007; Orlikowska and Schulz-Bull, 2009) are not considered because of the generally poor temporal data coverage. Fitting the in situ measurements onto our 1° × 1° grid leads on average to a reduction of the atmospheric mixing ratios and oceanic concentrations of less than 1 %. The accuracy of the interpolation is limited by the sparse data coverage and the regression technique used. Seasonal and spatial accuracy could be improved if a larger data set was available, thus we recommend more measurements, especially in the ocean, as well as a refinement of process understanding. The temporal variability of the SST is considered in the concentration gradient, used in the sea-to-air flux calculation, by computing a new equilibrium concentration for every 6 h time step from 1989–2011.

5.2 Annual and seasonal variability

The inter-annual variability of the global sea-to-air flux from 1989–2011 is small and generally less than 5 % (Fig. 7). The halocarbons show all a positive trend towards 2011. Within a year, the global flux varies monthly for every halogenated compound (Fig. 8). The maximum global sea-to-air flux is most pronounced in July for all compounds, while the minimum is reached in March–April for $CHBr_3$ and CH_3I and in October for CH_2Br_2. The climatological monthly flux and the corresponding minimum and maximum monthly fluxes vary between 9–21 %. CH_3I shows the smallest mean deviation with 9 and 11 % for OLS and RF respectively, whereas the variation for CH_2Br_2 is between 14 and 17 % and for $CHBr_3$ between 17 and 21 %. Thus the intra-annual variation of the global climatological flux is larger than the inter-annual variation, despite the shifting of the seasons (half a year) between the Northern and Southern Hemisphere. The largest influence on the global varying monthly sea-to-air fluxes have the tropics (20° S–20° N) for bromoform and dibromomethane, and the Southern Hemisphere for methyl iodide (not shown). The global climatological fluxes, obtained from the sum of the monthly averages between 1989 and 2011, describe the current best possible estimates of the moderately varying annual and seasonal global emissions.

5.3 Short time variability of fluxes

In situ fluxes from a cruise (TransBrom) between Japan and Australia (Quack et al., 2013) in October 2009 are compared to the nearest data points of our climatology (Fig. 9) as an example for the influence of short time variability. The cruise transited through different biogeochemical regions with varying meteorological conditions influencing the strength of VSLS emissions. The in situ and climatological sea-to-air fluxes for bromoform and dibromomethane compare very well in the Northern Hemisphere, where small concentration gradients are found in the open oceans. The enhanced emissions in the Southern Hemisphere, which are encountered during the cruise, are underrepresented in the climatology. Comparison of the methyl iodide in situ fluxes and the climatology shows a similar trend although the extreme values of the in situ measurements are highly underrepresented in the climatological mean flux value. Our climatology underestimates the short-term measured fluxes by smoothing the values of the varying input parameters. The mean deviation between the climatology and the in situ fluxes during October 2009 is ~ 120 % for $CHBr_3$, ~ 20 % for CH_2Br_2 and ~ 176 % for CH_3I, respectively.

We also calculate the sea-to-air fluxes using the nearest temporal and spatial 6 hourly means (highest available resolution) of SST, SLP and U, the monthly mean of the SSS and the climatological oceanic concentration and mixing ratios and compare them to the measured fluxes (Fig. 9). The mean deviation between the 6 hourly means and the in situ fluxes for the three compounds is only ~ 48 % for $CHBr_3$, ~ 15 % for CH_2Br_2 and 51 % for CH_3I. These values show the good match between "modeled" and in-situ measurements and validate the predictive capability of this approach. The climatological minimum and maximum values of the cruise nearest data points reveal how variable the "modeled" fluxes can be at a single location While most in-situ fluxes are included in the 6 h minimum and maximum range from 1989–2011, it is also noteworthy that even with this high temporal (6 h) resolution of input parameters, the "modeled" fluxes can neither match the extreme values of the encountered in situ fluxes, nor do they resolve the high variability of the in-situ fluxes completely. An additional factor for the underrepresentation of the extreme in-situ values is the mean concentration gradient (1° × 1° resolution) in our "model". In the vicinity of source regions, e.g. coast lines, the water concentrations can vary by more than 100 % over short distances (Butler et al., 2006; Quack et al., 2013), which strongly influences the in situ fluxes and is likely not resolved in the model due to poor data coverage.

6 Summary and conclusion

Global sea-to-air flux climatologies (considering the time span from 1989 to 2011 of the three important short-lived halocarbons, bromoform dibromomethane and methyl iodide) are calculated based on surface oceanic and atmospheric measurements from the HalOcAt database. Physical and biogeochemical factors of the compounds distributions in ocean and atmosphere are also considered. Data are classified into coastal, shelf and open ocean regions, and are interpolated on a 1° × 1° grid. The missing grid values are filled with Robust Fit (RF) and Ordinary Least Square (OLS) regression techniques based on the latitudinal and longitudinal distribution of the compounds. The RF interpolation estimates background values, since it is weighted on the quantity of measurements, whereas the OLS regressions include extreme data and therefore represent our upper-limit. Global emission fields are calculated with a high temporal resolution of

Title Page
Abstract Introduction
Conclusions References
Tables Figures
◀◀ ▶▶
◀ ▶
Back Close
Full Screen / Esc
Printer-friendly Version
Interactive Discussion

6 hourly wind speed, sea surface temperature and sea level pressure data. The climatological annual global flux for 1989 to 2011 is obtained as sum of the monthly average fluxes. We estimate positive global sea-to-air fluxes of $CHBr_3$, CH_2Br_2 and CH_3I of 2.06/2.96, 0.89/1.09 $\mathrm{Gmol\,Br\,yr^{-1}}$ and 1.24/1.45 $\mathrm{Gmol\,I\,yr^{-1}}$, based on RF and OLS respectively, which are all at the lower end of earlier studies. Previous global climatological estimate studies have not determined negative fluxes (flux into the ocean). We estimate negative global sea-to-air fluxes of −0.47/−0.56, −0.11/−0.12 $\mathrm{Gmol\,Br\,yr^{-1}}$ and −0.08/−0.1 $\mathrm{Mmol\,I\,yr^{-1}}$ for $CHBr_3$, CH_2Br_2 and CH_3I, respectively. The net oceanic emissions of our climatology are 1.5/2.5 $\mathrm{Gmol\,Br\,yr^{-1}}$ for $CHBr_3$, 0.78/0.98 $\mathrm{Gmol\,Br\,yr^{-1}}$, for CH_2Br_2 and 1.24/1.45 $\mathrm{Gmol\,I\,yr^{-1}}$ for CH_3I.

Our low bottom up emission estimates, compared to recent top down approaches, especially for bromoform, are most likely caused by an underrepresentation of extreme emissions. Observed high temporal and spatial in situ variances cannot be resolved in the $1^\circ \times 1^\circ$ grid climatology. It is still unclear how important extreme events for the global bromoform budget are, but we suggest that short temporal events of high oceanic bromoform emissions on small spatial and temporal scales are important for the transport of bromine into the troposphere and lower stratosphere. The monthly variation of the global climatological flux (9–21 %) is contained within our calculations and it is larger than the inter-annual variation, which is generally less than 5 % for all three compounds.

Our global sea-to-air flux estimates will improve the quantification of the oceanic contribution to the impact of brominated and iodinated short-lived substances on global (future) climate and ozone depletion. The existing uncertainties can be reduced by enlarging of the HalOcAt data base with more measurements, especially in ocean waters, common calibration techniques and more basic research into the underlying source and sink processes.

Supplementary material related to this article is available online at: http://www.atmos-chem-phys-discuss.net/13/5601/2013/acpd-13-5601-2013-supplement.zip.

Acknowledgements. We thank all contributors sending their data to the HalOcAt database and for their helpful comments on the manuscript. We also thank our assisting student helpers Julian Kinzel, Christian Müller, Eike Hümpel, Anja Müller and Theresa Conradi who populated the database, which started in 2009. This work was financially supported by the WGL project Transbrom, the European commission under the project SHIVA (grant no. 226 224) and by the German Federal Ministry of Education and Research (BMBF) during the project SOPRAN (grant no: 03F0611A). SOLAS Integration (Surface Ocean Lower Atmosphere Study; http://www.bodc.ac.uk/solas_integration/) helped instigate this project and Tom Bell and Peter Liss were supported in this by a NERC UK SOLAS Knowledge Transfer grant (NE/E001696/1). Part of this project was supported by COST (Cooperation in the field of Scientific and Technical Research) Action 735, a European Science Foundation-supported initiative. Additionally, we would like to thank the ECMWF for providing the ERA Interim reanalysis data.

The service charges for this open access publication
have been covered by a Research Centre of the
Helmholtz Association.

References

Abrahamsson, K., Bertilsson, S., Chierici, M., Fransson, A., Froneman, P. W., Loren, A., and Pakhomov, E. A.: Variations of biochemical parameters along a transect in the Southern Ocean, with special emphasis on volatile halogenated organic compounds, Deep-Sea Res. Pt. II, 51, 2745–2756, doi:10.1016/j.dsr2.2004.09.004, 2004.

Amachi, S., Kamagata, Y., Kanagawa, T., and Muramatsu, Y.: Bacteria mediate methylation of iodine in marine and terrestrial environments, Appl. Environ. Microb., 67, 2718–2722, doi:10.1128/aem.67.6.2718-2722.2001, 2001.

Antonov, J. I., Seidov, D., Boyer, T. P., Locarnini, R. A., Mishonov, A. V., Garcia, H. E., Baranova, O. K., Zweng, M. M., and Johnson, D. R.: Salinity, vol. 2, in: World Ocean Atlas 2009, edited by: Levitus, S., NOAA Atlas NESDIS 69, US Government Printing Office, Washington, D.C., 184 pp., 2010.

Archer, S. D., Goldson, L. E., Liddicoat, M. I., Cummings, D. G., and Nightingale, P. D.: Marked seasonality in the concentrations and sea-to-air flux of volatile iodocarbon compounds in the western English Channel, J. Geophys. Res.-Oceans, 112, C08009, doi:10.1029/2006jc003963, 2007.

Aschmann, J., Sinnhuber, B.-M., Atlas, E. L., and Schauffler, S. M.: Modeling the transport of very short-lived substances into the tropical upper troposphere and lower stratosphere, Atmos. Chem. Phys., 9, 9237–9247, doi:10.5194/acp-9-9237-2009, 2009.

Bates, N. R. and Merlivat, L.: The influence of short-term wind variability on air-sea CO_2 exchange, Geophys. Res. Lett., 28, 3281–3284, doi:10.1029/2001gl012897, 2001.

Bell, N., Hsu, L., Jacob, D. J., Schultz, M. G., Blake, D. R., Butler, J. H., King, D. B., Lobert, J. M., and Maier-Reimer, E.: Methyl iodide: atmospheric budget and use as a tracer of marine convection in global models, J. Geophys. Res.-Atmos., 107, 4340, doi:10.1029/2001jd001151, 2002.

Bondu, S., Cocquempot, B., Deslandes, E., and Morin, P.: Effects of salt and light stress on the release of volatile halogenated organic compounds by *Solieria Chordalis*: a laboratory incubation study, Bot. Mar., 51, 485–492, doi:10.1515/bot.2008.056, 2008.

Brownell, D. K., Moore, R. M., and Cullen, J. J.: Production of methyl halides by *Prochlorococcus* and *Synechococcus*, Global Biogeochem. Cy., 24, GB2001, doi:10.1029/2009gb003671, 2010.

Butler, J. H., King, D. B., Lobert, J. M., Montzka, S. A., Yvon-Lewis, S. A., Hall, B. D., Warwick, N. J., Mondeel, D. J., Aydin, M., and Elkins, J. W.: Oceanic distributions and emissions of short-lived halocarbons, Global Biogeochem. Cy., 21, GB1023, doi:10.1029/2006gb002732, 2007.

Butler, J. H., Bell, T. G., Hall, B. D., Quack, B., Carpenter, L. J., and Williams, J.: Technical Note: Ensuring consistent, global measurements of very short-lived halocarbon gases in the ocean and atmosphere, Atmos. Chem. Phys., 10, 327–330, doi:10.5194/acp-10-327-2010, 2010.

Carpenter, L. J.: Iodine in the marine boundary layer, Chem. Rev., 103, 4953–4962, doi:10.1021/cr0206465, 2003.

Carpenter, L. J. and Liss, P. S.: On temperate sources of bromoform and other reactive organic bromine gases, J. Geophys. Res.-Atmos., 105, 20539–20547, doi:10.1029/2000jd900242, 2000.

Chapman, E. G., Shaw, W. J., Easter, R. C., Bian, X., and Ghan, S. J.: Influence of wind speed averaging on estimates of dimethylsulfide emission fluxes, J. Geophys. Res.-Atmos., 107, 4672, doi:10.1029/2001jd001564, 2002.

Chipperfield, M. P. and Pyle, J. A.: Model sensitivity studies of arctic ozone depletion, J. Geophys. Res.-Atmos., 103, 28389–28403, doi:10.1029/98jd01960, 1998.

Daley, R.: Atmospheric Data Analysis, Cambridge University Press, Cambridge, England, 457 pp., 1991.

Dee, D. P., Uppala, S. M., Simmons, A. J., Berrisford, P., Poli, P., Kobayashi, S., Andrae, U., Balmaseda, M. A., Balsamo, G., Bauer, P., Bechtold, P., Beljaars, A. C. M., van de Berg, L., Bidlot, J., Bormann, N., Delsol, C., Dragani, R., Fuentes, M., Geer, A. J., Haimberger, L., Healy, S. B., Hersbach, H., Hólm, E. V., Isaksen, L., Kållberg, P., Köhler, M., Matricardi, M., McNally, A. P., Monge-Sanz, B. M., Morcrette, J.-J., Park, B.-K., Peubey, C., de Rosnay, P., Tavolato, C., Thépaut, J.-N., and Vitart, F.: The era-interim reanalysis: configuration and performance of the data assimilation system, Q. J. Roy. Meteor. Soc., 137, 553–597, doi:10.1002/qj.828, 2011.

Dorf, M., Butz, A., Camy-Peyret, C., Chipperfield, M. P., Kritten, L., and Pfeilsticker, K.: Bromine in the tropical troposphere and stratosphere as derived from balloon-borne BrO observations, Atmos. Chem. Phys., 8, 7265–7271, doi:10.5194/acp-8-7265-2008, 2008.

Gschwend, P. M., Mac Farlane, J. K., and Newman, K. A.: Volatile halogenated organic-compounds released to seawater from temperate marine macro algae, Science, 227, 1033–1035, doi:10.1126/science.227.4690.1033, 1985.

Hagen, E., Feistel, R., Agenbag, J. J., and Ohde, T.: Seasonal and interannual changes in intense Benguela upwelling (1982–1999), Oceanol. Acta, 24, 557–568, doi:10.1016/s0399-1784(01)01173-2, 2001.

Happell, J. D. and Wallace, D. W. R.: Methyl iodide in the Greenland/Norwegian seas and the tropical Atlantic Ocean: evidence for photochemical production, Geophys Res. Lett., 23, 2105–2108, doi:10.1029/96gl01764, 1996.

Huber, P. J.: Robust estimation of location parameter, Ann. Math. Stat., 35, 73–101, doi:10.1214/aoms/1177703732, 1964.

Hughes, C., Chuck, A. L., Rossetti, H., Mann, P. J., Turner, S. M., Clarke, A., Chance, R., and Liss, P. S.: Seasonal cycle of seawater bromoform and dibromomethane concentrations in a coastal bay on the western Antarctic Peninsula, Global Biogeochem. Cy., 23, GB2024, doi:10.1029/2008gb003268, 2009.

Hughes, C., Franklin, D. J., and Malin, G.: Iodomethane production by two important marine cyanobacteria: *Prochlorococcus marinus* (ccmp 2389) and *Synechococcus sp* (ccmp 2370), Mar. Chem., 125, 19–25, doi:10.1016/j.marchem.2011.01.007, 2011.

Johnson, M. T.: A numerical scheme to calculate temperature and salinity dependent air-water transfer velocities for any gas, Ocean Sci., 6, 913–932, doi:10.5194/os-6-913-2010, 2010.

Jones, C. E., Andrews, S. J., Carpenter, L. J., Hogan, C., Hopkins, F. E., Laube, J. C., Robinson, A. D., Spain, T. G., Archer, S. D., Harris, N. R. P., Nightingale, P. D., O'Doherty, S. J., Oram, D. E., Pyle, J. A., Butler, J. H., and Hall, B. D.: Results from the first national UK inter-laboratory calibration for very short-lived halocarbons, Atmos. Meas. Tech., 4, 865–874, doi:10.5194/amt-4-865-2011, 2011.

Kerkweg, A., Jöckel, P., Warwick, N., Gebhardt, S., Brenninkmeijer, C. A. M., and Lelieveld, J.: Consistent simulation of bromine chemistry from the marine boundary layer to the stratosphere – Part 2: Bromocarbons, Atmos. Chem. Phys., 8, 5919–5939, doi:10.5194/acp-8-5919-2008, 2008.

Kettle, H. and Merchant, C. J.: Systematic errors in global air-sea CO_2 flux caused by temporal averaging of sea-level pressure, Atmos. Chem. Phys., 5, 1459–1466, doi:10.5194/acp-5-1459-2005, 2005.

Ko, M. K. W., Poulet, G., Blake, D. R., Boucher, O., Burkholder, J. H., Chin, M., Cox, R. A., George, C., Graf, H.-F., Holton, J. R., Jacob, D. J., Law, K. S., Lawrence, M. G., Midgley, P. M., Seakins, P. W., Shallcross, D. E., Strahan, S. E., Wuebbles, D. J., and Yokouchi, Y.: Very short-lived halogen and sulfur substances, in: Scientific Assessment of Ozone Depletion: 2002, Global Ozone Res. Monit. Proj. Rep. 47, World Meteorol. Org., Geneva, 2.1–2.57, 2003.

Laturnus, F., Adams, F. C., and Wiencke, C.: Methyl halides from Antarctic macro algae, Geophys. Res. Lett., 25, 773–776, doi:10.1029/98gl00490, 1998.

Liang, Q., Stolarski, R. S., Kawa, S. R., Nielsen, J. E., Douglass, A. R., Rodriguez, J. M., Blake, D. R., Atlas, E. L., and Ott, L. E.: Finding the missing stratospheric Br_y: a global modeling study of $CHBr_3$ and CH_2Br_2, Atmos. Chem. Phys., 10, 2269–2286, doi:10.5194/acp-10-2269-2010, 2010.

Liss, P. S. and Merlivat, L.: Air-sea gas exchange rates: introduction and synthesis, in: The Role of Air-Sea Exchange in Geochemical Cycling, edited by: Buat-Ménard, P. and Reidel, D., Hingham, Mass., 113–129, 1986.

Liu, Y., Yvon-Lewis, S. A., Hu, L., Salisbury, J. E., and O'Hern, J. E.: $CHBr_3$, CH_2Br_2, and $CHClBr_2$ in U.S. coastal waters during the Gulf of Mexico and East Coast carbon cruise, J. Geophys. Res., 116, C10004, doi:10.1029/2010JC006729, 2011.

Manley, S. L. and Dastoor, M. N.: Methyl-iodide (CH_3I) production by kelp and associated microbes, Mar. Biol., 98, 477–482, doi:10.1007/bf00391538, 1988.

Manley, S. L. and delaCuesta, J. L.: Methyl iodide production from marine phytoplankton cultures, Limnol. Oceanogr., 42, 142–147, 1997.

Manley, S. L., Goodwin, K., and North, W. J.: Laboratory production of bromoform, methylene bromide, and methyl-iodide by macro algae and distribution in near-shore southern California waters, Limnol. Oceanogr., 37, 1652–1659, 1992.

McFiggans, G., Plane, J. M. C., Allan, B. J., Carpenter, L. J., Coe, H., and O'Dowd, C.: A modeling study of iodine chemistry in the marine boundary layer, J. Geophys. Res.-Atmos., 105, 14371–14385, doi:10.1029/1999jd901187, 2000.

Minas, H. J., Packard, T. T., Minas, M., and Coste, B.: An analysis of the production-regeneration system in the coastal upwelling area off NW Africa based on oxygen, nitrate and ammonium distributions, J. Mar. Res., 40, 615–641, 1982.

Montzka, S. A. and Reimann, S.: Ozone-depleting substances and related chemicals, in: Scientific Assessment of Ozone Depletion: 2010, Global Ozone Research and Monitoring Project – Report No. 52, chapt. 1, edited by: World Meteorological Project, Geneva, Switzerland, 2011.

Moore, R. M. and Zafiriou, O. C.: Photochemical production of methyl-iodide in seawater, J. Geophys. Res.-Atmos., 99, 16415–16420, doi:10.1029/94jd00786, 1994.

Moore, R. M., Geen, C. E., and Tait, V. K.: Determination of Henry law constants for a suite of naturally-occurring halogenated methanes in seawater, Chemosphere, 30, 1183–1191, doi:10.1016/0045-6535(95)00009-w, 1995a.

Moore, R. M., Tokarczyk, R., Tait, V. K., Poulin, M., and and Geen, C. E.: Marine phytoplankton as a natural source of volatile organohalogens, in: Naturally-Produced Organohalogens, edited by: Grimvall, A. and deLeer, E. W. B., Kluwer Academic Publishers, Dordrecht, 283–294, 1995b.

Nightingale, P. D., Malin, G., and Liss, P. S.: Production of chloroform and other low-molecular-weight halocarbons by some species of macro algae, Limnol. Oceanogr., 40, 680–689, 1995.

Nightingale, P. D., Malin, G., Law, C. S., Watson, A. J., Liss, P. S., Liddicoat, M. I., Boutin, J., and Upstill-Goddard, R. C.: In situ evaluation of air-sea gas exchange parameterizations using novel conservative and volatile tracers, Global Biogeochem. Cy., 14, 373–387, 2000.

O'Brien, L. M., Harris, N. R. P., Robinson, A. D., Gostlow, B., Warwick, N., Yang, X., and Pyle, J. A.: Bromocarbons in the tropical marine boundary layer at the Cape

Verde Observatory – measurements and modelling, Atmos. Chem. Phys., 9, 9083–9099, doi:10.5194/acp-9-9083-2009, 2009.

Ordóñez, C., Lamarque, J.-F., Tilmes, S., Kinnison, D. E., Atlas, E. L., Blake, D. R., Sousa Santos, G., Brasseur, G., and Saiz-Lopez, A.: Bromine and iodine chemistry in a global chemistry-climate model: description and evaluation of very short-lived oceanic sources, Atmos. Chem. Phys., 12, 1423–1447, doi:10.5194/acp-12-1423-2012, 2012.

Orlikowska, A. and Schulz-Bull, D. E.: Seasonal variations of volatile organic compounds in the coastal Baltic sea, Environ. Chem., 6, 495–507, doi:10.1071/en09107, 2009.

Penkett, S. A., Jones, B. M. R., Rycroft, M. J., and Simmons, D. A.: An interhemispheric comparison of the concentrations of bromine compounds in the atmosphere, Nature, 318, 550–553, doi:10.1038/318550a0, 1985.

Pyle, J. A., Ashfold, M. J., Harris, N. R. P., Robinson, A. D., Warwick, N. J., Carver, G. D., Gostlow, B., O'Brien, L. M., Manning, A. J., Phang, S. M., Yong, S. E., Leong, K. P., Ung, E. H., and Ong, S.: Bromoform in the tropical boundary layer of the Maritime Continent during OP3, Atmos. Chem. Phys., 11, 529–542, doi:10.5194/acp-11-529-2011, 2011.

Quack, B. and Wallace, D. W. R.: Air-sea flux of bromoform: controls, rates, and implications, Global Biogeochem. Cy., 17, 1023, doi:10.1029/2002gb001890, 2003.

Quack, B., Atlas, E., Petrick, G., Stroud, V., Schauffler, S., and Wallace, D. W. R.: Oceanic bromoform sources for the tropical atmosphere, Geophys. Res. Lett., 31, L23S05, doi:10.1029/2004gl020597, 2004.

Quack, B., Atlas, E., Petrick, G., and Wallace, D. W. R.: Bromoform and dibromomethane above the Mauritanian upwelling: atmospheric distributions and oceanic emissions, J. Geophys. Res.-Atmos., 112, D09312, doi:10.1029/2006jd007614, 2007a.

Quack, B., Peeken, I., Petrick, G., and Nachtigall, K.: Oceanic distribution and sources of bromoform and dibromomethane in the Mauritanian upwelling, J. Geophys. Res.-Oceans, 112, C10006, doi:10.1029/2006jc003803, 2007b.

Quack, B., Atlas, E., Krüger, K., Taylor, B., Dinter, T., Bracher, A., Petrick, G., Stange, K., Fuhlbrügge, S., Tegtmeier, S., Wache, S., and Wallace, D.: Distribution and air-sea fluxes of halocarbons through the Western Pacific, in preparation, 2013.

Richter, U. and Wallace, D. W. R.: Production of methyl iodide in the tropical Atlantic Ocean, Geophys. Res. Lett., 31, L23S03, doi:10.1029/2004gl020779, 2004.

Salawitch, R. J., Weisenstein, D. K., Kovalenko, L. J., Sioris, C. E., Wennberg, P. O., Chance, K., Ko, M. K. W., and McLinden, C. A.: Sensitivity of ozone to bromine in the lower stratosphere, Geophys. Res. Lett., 32, L05811, doi:10.1029/2004gl021504, 2005.

Schott, F. A., Dengler, M., and Schoenefeldt, R.: The shallow overturning circulation of the Indian Ocean, Prog. Oceanogr., 53, 57–103, doi:10.1016/s0079-6611(02)00039-3, 2002.

Sinnhuber, B.-M. and Folkins, I.: Estimating the contribution of bromoform to stratospheric bromine and its relation to dehydration in the tropical tropopause layer, Atmos. Chem. Phys., 6, 4755–4761, doi:10.5194/acp-6-4755-2006, 2006.

Sinnhuber, B.-M., Sheode, N., Sinnhuber, M., Chipperfield, M. P., and Feng, W.: The contribution of anthropogenic bromine emissions to past stratospheric ozone trends: a modelling study, Atmos. Chem. Phys., 9, 2863–2871, doi:10.5194/acp-9-2863-2009, 2009.

Sive, B. C., Varner, R. K., and Mao, H.: A large terrestrial source of methyl iodide, Geophys. Res. Lett., 20, L17808, doi:10.1029/2007GL030528, 2007.

Smith, W. O. and Nelson, D. M.: Phytoplankton bloom produced by a receding ice edge in the Ross Sea – spatial coherence with the density field, Science, 227, 163–166, doi:10.1126/science.227.4683.163, 1985.

Smythe-Wright, D., Boswell, S. M., Breithaupt, P., Davidson, R. D., Dimmer, C. H., and Diaz, L. B. E.: Methyl iodide production in the ocean: implications for climate change, Global Biogeochem. Cy., 20, GB3003, doi:10.1029/2005gb002642, 2006.

Solomon, S., Garcia, R. R., and Ravishankara, A. R.: On the role of iodine in ozone depletion, J. Geophys. Res.-Atmos., 99, 20491–20499, doi:10.1029/94jd02028, 1994.

Sturges, W. T., Oram, D. E., Carpenter, L. J., Penkett, S. A., and Engel, A.: Bromoform as a source of stratospheric bromine, Geophys. Res. Lett., 27, 2081–2084, doi:10.1029/2000gl011444, 2000.

Tegtmeier, S., Krüger, K., Quack, B., Atlas, E. L., Pisso, I., Stohl, A., and Yang, X.: Emission and transport of bromocarbons: from the West Pacific ocean into the stratosphere, Atmos. Chem. Phys., 12, 10633–10648, doi:10.5194/acp-12-10633-2012, 2012.

Tokarczyk, R. and Moore, R. M.: Production of volatile organohalogens by phytoplankton cultures, Geophys. Res. Lett., 21, 285–288, doi:10.1029/94gl00009, 1994.

Vogt, R., Sander, R., Von Glasow, R., and Crutzen, P. J.: Iodine chemistry and its role in halogen activation and ozone loss in the marine boundary layer: a model study, J. Atmos. Chem., 32, 375–395, doi:10.1023/a:1006179901037, 1999.

von Glasow, R.: Atmospheric chemistry – sun, sea and ozone destruction, Nature, 453, 1195–1196, doi:10.1038/4531195a, 2008.

von Glasow, R., von Kuhlmann, R., Lawrence, M. G., Platt, U., and Crutzen, P. J.: Impact of reactive bromine chemistry in the troposphere, Atmos. Chem. Phys., 4, 2481–2497, doi:10.5194/acp-4-2481-2004, 2004.

Wanninkhof, R.: Relationship between wind-speed and gas-exchange over the ocean, J. Geophys. Res.-Oceans, 97, 7373–7382, doi:10.1029/92jc00188, 1992.

Wanninkhof, R. and McGillis, W. R.: A cubic relationship between air-sea CO_2 exchange and wind speed, Geophys. Res. Lett., 26, 1889–1892, doi:10.1029/1999gl900363, 1999.

Warneck, P. and Williams, J.: The Atmospheric Chemist's Companion-Numerical Data for use in the Atmospheric Sciences, Springer Science + Business Media B.V., 2012.

Warwick, N. J., Pyle, J. A., Carver, G. D., Yang, X., Savage, N. H., O'Connor, F. M., and Cox, R. A.: Global modeling of biogenic bromocarbons, J. Geophys. Res.-Atmos., 111, D24305, doi:10.1029/2006jd007264, 2006.

Williams, J., Gros, V., Atlas, E., Maciejczyk, K., Batsaikhan, A., Scholer, H. F., Forster, C., Quack, B., Yassaa, N., Sander, R., and Van Dingenen, R.: Possible evidence for a connection between methyl iodide emissions and Saharan dust, J. Geophys. Res.-Atmos., 112, D07302, doi:10.1029/2005jd006702, 2007.

Yamamoto, H., Yokouchi, Y., Otsuki, A., and Itoh, H.: Depth profiles of volatile halogenated hydrocarbons in seawater in the Bay of Bengal, Chemosphere, 45, 371–377, doi:10.1016/s0045-6535(00)00541-5, 2001.

Yokouchi, Y., Mukai, H., Yamamoto, H., Otsuki, A., Saitoh, C., and Nojiri, Y.: Distribution of methyl iodide, ethyl iodide, bromoform, and dibromomethane over the ocean (east and Southeast Asian seas and the western pacific), J. Geophys. Res.-Atmos., 102, 8805–8809, doi:10.1029/96jd03384, 1997.

Yokouchi, Y., Hasebe, F., Fujiwara, M., Takashima, H., Shiotani, M., Nishi, N., Kanaya, Y., Hashimoto, S., Fraser, P., Toom-Sauntry, D., Mukai, H., and Nojiri, Y.: Correlations and emission ratios among bromoform, dibromochloromethane, and dibromomethane in the atmosphere, J. Geophys. Res.-Atmos., 110, D23309, doi:10.1029/2005jd006303, 2005.

Yokouchi, Y., Osada, K., Wada, M., Hasebe, F., Agama, M., Murakami, R., Mukai, H., Nojiri, Y., Inuzuka, Y., Toom-Sauntry, D., and Fraser, P.: Global distribution and seasonal concentration change of methyl iodide in the atmosphere, J. Geophys. Res.-Atmos., 113, D18311, doi:10.1029/2008jd009861, 2008.

Table 1. Statistical moments; mean (μ), median, standard deviation (σ), minimum and maximum value of atmospheric mixing ratio (ppt) and oceanic concentration ($\mathrm{pmol\,L^{-1}}$) climatologies of $CHBr_3$, CH_2Br_2 and CH_3I based on the RF and OLS regression analyses.

Compound	μ		Median		σ		Minimum		Maximum	
	RF	OLS	RF	OLS	RF	OLS	RF	OLS	RF	OLS
Atmosphere										
$CHBr_3$	0.9	1.1	1.0	1.6	1.2	1.6	0.01	0.03	53.1	53.1
CH_2Br_2	1.0	1.1	1.0	1.1	0.4	0.4	0.07	0.07	7.8	7.8
CH_3I	0.7	0.8	0.7	0.7	0.4	0.4	0.05	0.01	7.3	7.3
Ocean										
$CHBr_3$	5.9	9.3	3.1	4.4	9.8	14.6	0.29	0.19	823.0	823.0
CH_2Br_2	2.9	3.5	1.9	2.6	2.4	2.7	0.01	0.01	89.8	89.8
CH_3I	3.2	3.9	2.6	3.4	2.6	2.9	0.03	0.05	39.6	39.6

Table 2. Statistical moments; mean (µ), median, standard deviation (σ), minimum and maximum value for the calculated global sea-to-air flux climatology; $CHBr_3$, CH_2Br_2 and CH_3I based on the RF and OLS regression analyses in pmol m^{-2} h^{-1}.

Global sea-to-air	µ		Median		σ		Minimum		Maximum	
flux climatology	RF	OLS	RF	OLS	RF	OLS	RF	OLS	RF	OLS
$CHBr_3$	154.9	236.2	47.1	89.7	549.7	749.6	−5339	−5230	19 618	19 618
CH_2Br_2	76.5	112.4	79.3	78.8	237.9	258.4	−1687	−1714	3978	3978
CH_3I	329.6	405.0	307.3	385.2	289.8	348.3	−49	−55	4895	4878

Title Page
Abstract Introduction
Conclusions References
Tables Figures
◀| |▶
◀ ▶
Back Close
Full Screen / Esc
Printer-friendly Version
Interactive Discussion

Table 3. Percentage emission distribution of $CHBr_3$, CH_2Br_2 and CH_3I calculated with two different regression methods (RF and OLS) (see text for explanation).

	$CHBr_3$		CH_2Br_2		CH_3I	
	RF	OLS	RF	OLS	RF	OLS
50–90° N	22.8	21.2	−9.7	−4.9	10.4	7.6
20–50° N	7.4	15.9	13.7	19.1	19.8	20.3
20° N–20° S	54.7	43.6	48.9	44.3	28.9	32.1
20–50° S	22.7	19.3	25.1	22.1	32.8	34.1
50–90° S	−7.6	0.007	22.0	19.5	8.2	5.9

Table 4. Fluxes of bromine from $CHBr_3$ and CH_2Br_2 in $\mathrm{Gmol\,Br\,yr^{-1}}$, and iodine from CH_3I in $\mathrm{Gmol\,I\,yr^{-1}}$.

References	$CHBr_3$ flux ($\mathrm{Gmol\,Br\,yr^{-1}}$) Global		CH_2Br_2 flux ($\mathrm{Gmol\,Br\,yr^{-1}}$) Global		CH_3I flux ($\mathrm{Gmol\,I\,yr^{-1}}$) Global		Approach
Butler et al. (2007)	10.01		3.50		4.33		bottom up
Liang et al. (2010)	5.38		0.71				top down
O'Brien et al. (2009)	10.26						bottom up
Yokouchi et al. (2005)	10.26						bottom up
Warwick et al. (2006)	7.01		1.25				top down
Quack and Wallace (2003)	10.01						bottom up
Smythe-Wright et al. (2006)					4.18		labexperiment
Bell et al. (2002)					2.4		model study
Ordonez et al. (2011)	6.67		0.84		2.39		top down
Kerkweg et al. (2008)	7.45		1.41				top down
	source	sink	source	sink	source	sink	
This study RF	2.06	−0.56	0.89	−0.12	1.24	−0.00008	bottom up
This study OLS	2.96	−0.47	1.09	−0.11	1.45	−0.0001	bottom up

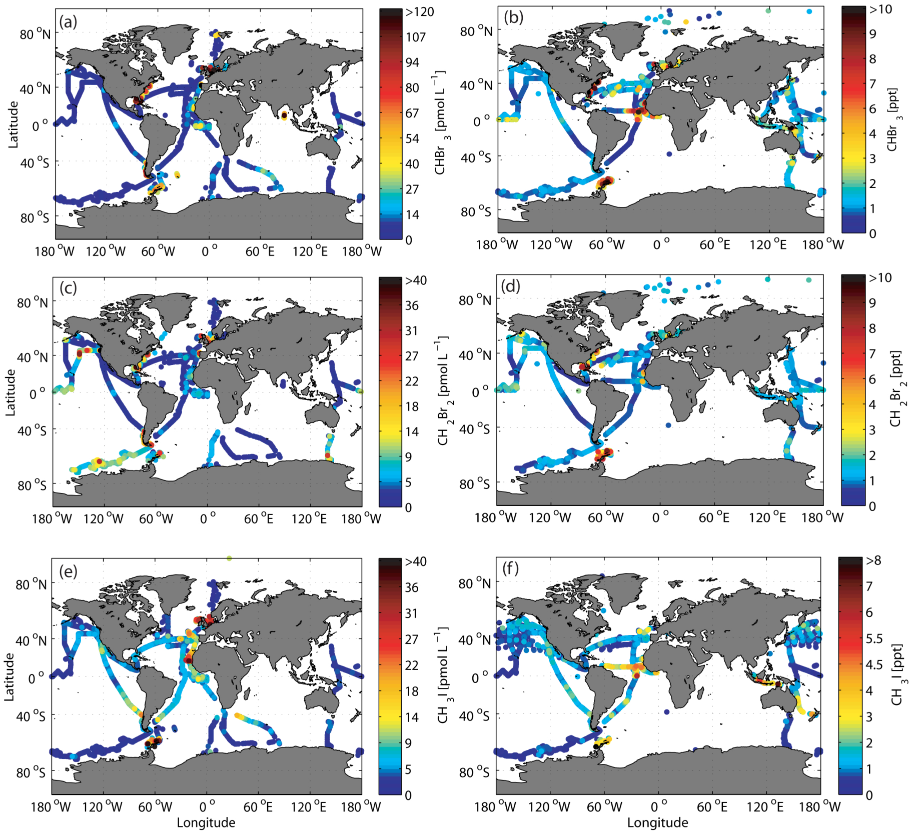

Fig. 1. Global coverage of available surface seawater measurements in pmol L^{-1} and atmospheric measurements in ppt for bromoform **(a, b)**, dibromomethane **(c, d)** and methyl iodide **(e, f)** from the HalOcAt database project.

Title Page
Abstract | Introduction
Conclusions | References
Tables | Figures
◀| |▶
◀ ▶
Back | Close
Full Screen / Esc
Printer-friendly Version
Interactive Discussion

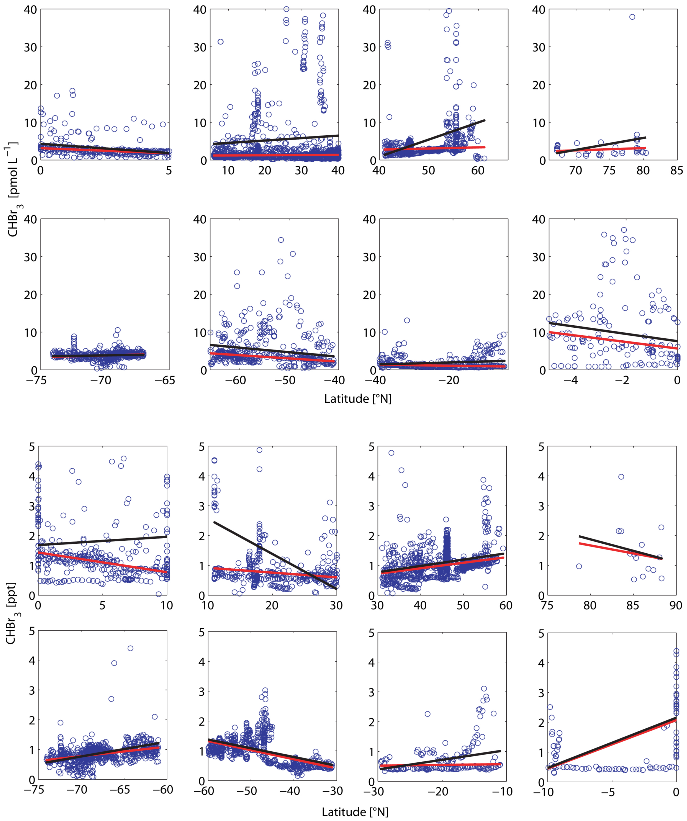

Fig. 2. Latitudinal distribution of open ocean water (upper panels) in pmol L^{-1} and atmosphere (lower panels) in ppt bromoform concentrations (blue circles) classified in eight different latitudinal bands. The Robust Fit (RF) (red line) and Ordinary Least Square (OLS) (black line) regression analyses are included.

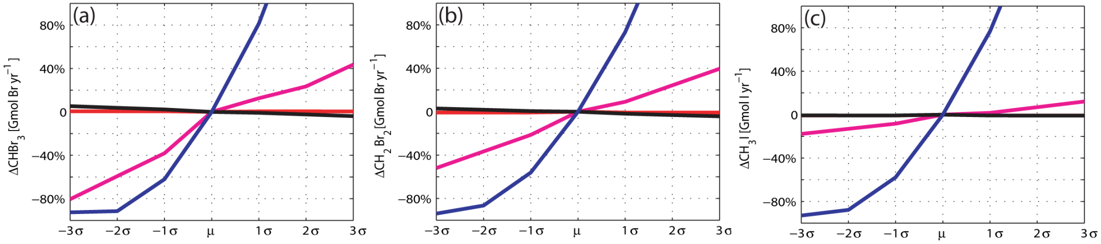

Fig. 3. The percentage change of the global oceanic emission for bromoform **(a)**, dibromomethane **(b)**, both in Gmol Br yr^{-1}, and methyl iodide **(c)** in Gmol I yr^{-1} based on individual input parameters: wind speed (blue), sea surface temperature (magenta), sea surface salinity (red) and sea level pressure (black). The input parameters are individually increased and decreased by their multiple standard deviations (−3σ to 3σ) while holding the other ones fixed (μ presents the oceanic emission using the mean input parameters).

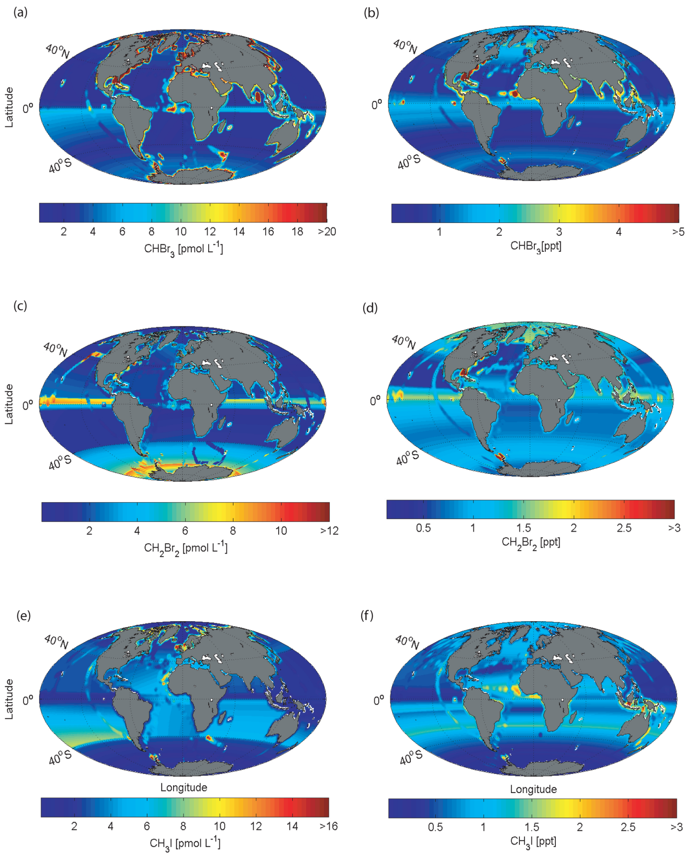

Fig. 4. Global maps of marine concentrations (pmol L^{-1}) and atmospheric mixing ratios (ppt) for bromoform **(a, b)**, dibromomethane **(c, d)** and methyl iodide **(e, f)** based on the Robust Fit (RF) regression analyses. The concentration maps calculated with the OLS method are included in the Supplement (Fig. S3).

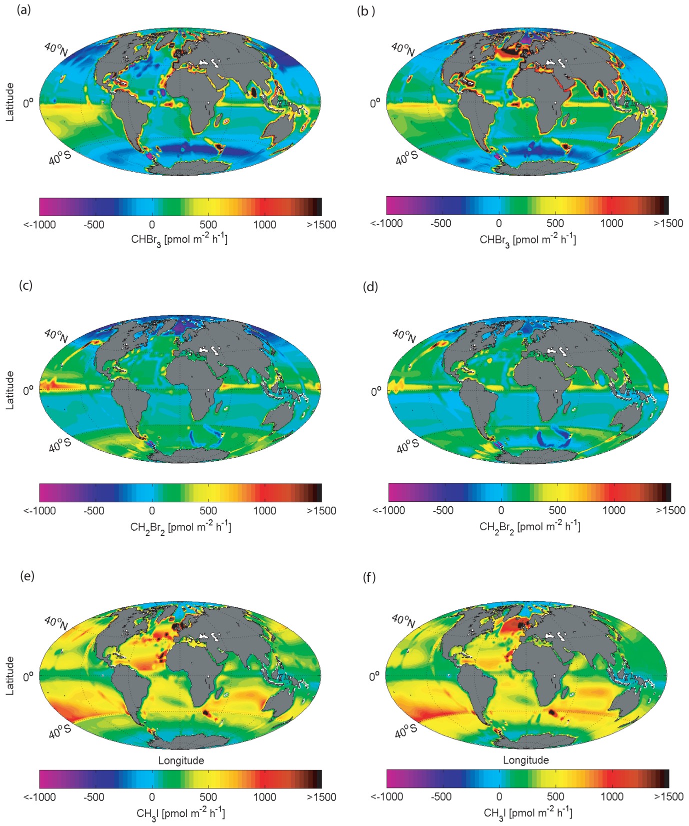

Fig. 5. Global sea-to-air flux climatology of bromoform **(a, b)**, dibromomethane **(c, d)** and methyl iodide **(e, f)** in pmol m^{-2} h^{-1} based on the RF (**a**, **c**, **e**, left column) and OLS (**b**, **d**, **f**, right column) analyses.

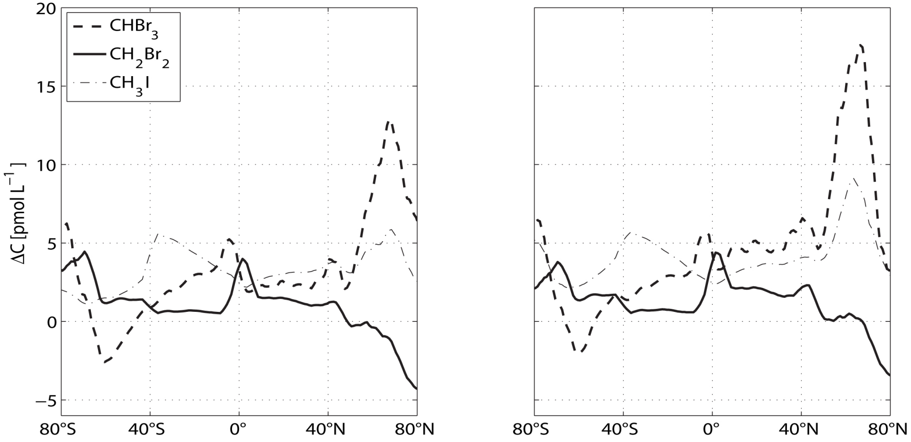

Fig. 6. Zonal mean concentration gradients for bromoform (dashed line), dibromomethane (solid line) and methyl iodide (dash-dotted line) in pmol L^{-1}, calculated with RF (left side) and OLS (right side) method.

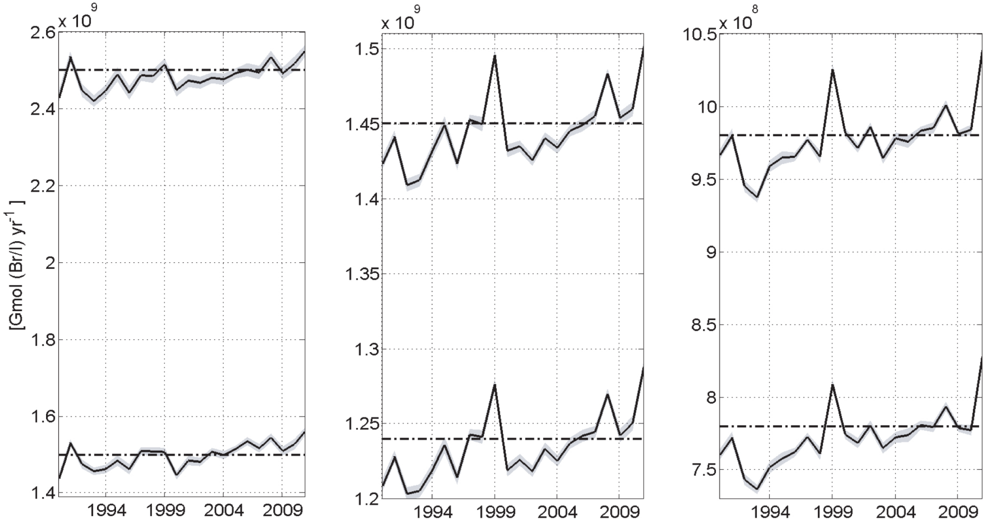

Fig. 7. Inter-annual sea-to-air flux variability over 1989–2011 (bold solid line) of bromoform (left), dibromomethane (centre) and methyl iodide (right) calculated with the two regression techniques (RF (lower panels) and OLS (upper panels)) in Gmol (Br/I) yr^{-1}. Additionally, the respective climatological value is marked (dash-dotted line) as well as the standard deviation (grey shaded).

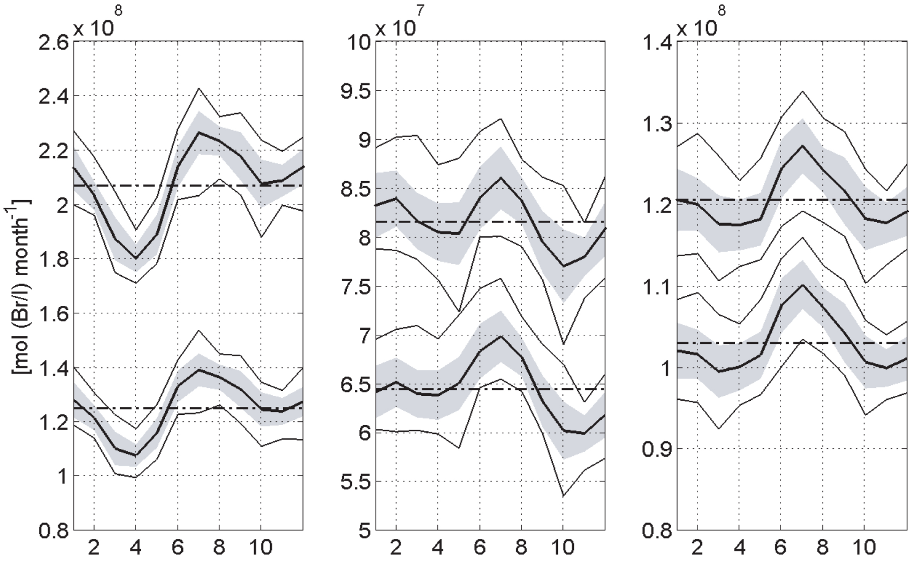

Fig. 8. Global monthly sea-to-air flux averages of bromoform (left), dibromomethane (centre) and methyl iodide (right) in mol (Br/I) month^{-1} (bold solid line) from 1989–2011 including their standard deviation (grey shaded area) and their minimum and maximum value (solid line). Additionally, the respective annual mean value is marked (dash-dotted line). The upper graphs show the oceanic emissions using the OLS regression technique and the bottom graphs the RF calculated fluxes.

Title Page
Abstract
Introduction
Conclusions
References
Tables
Figures
◀I
▶I
◀
▶
Back
Close
Full Screen / Esc
Printer-friendly Version
Interactive Discussion

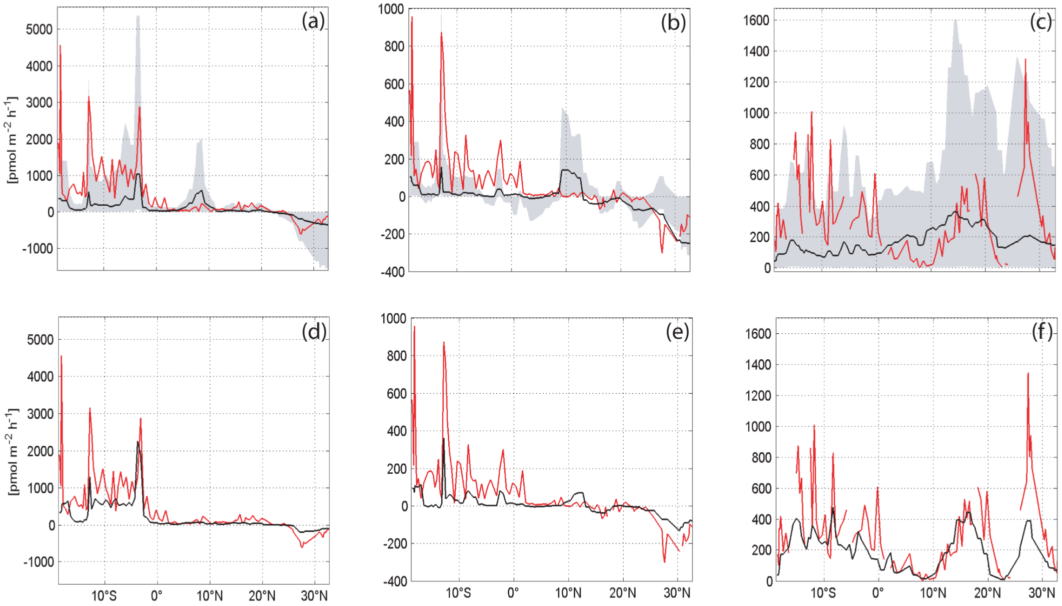

Fig. 9. The upper panels illustrate the comparison between our climatology estimate (black line) and in situ sea-to-air fluxes from the TransBrom cruise (red line) for bromoform **(a)**, dibromomethane **(b)** and methyl iodide **(c)** in pmol m^{-2} h^{-1} (see more details in text) including the climatological minimum and maximum values (grey shaded area). The lower panels represent the same in situ measurements compared to our model values using the nearest 6 hourly mean of SST, *U* and SLP and monthly mean of SSS with fixed mixing ratios and oceanic concentrations calculated with the RF method for bromoform **(d)**, dibromomethane **(e)** and methyl iodide **(f)** (the emissions using OLS look similar).